Crystallization and Melting Behavior of Poly (L-lactic Acid)

Takahiko Kawai,*,† Nelly Rahman,† Go Matsuba,† Koji Nishida,† Toshiji Kanaya,† Mitsuru Nakano,‡ Hirotaka Okamoto,‡ Jumpei Kawada,‡ Arimitsu Usuki,‡ Nobutaka Honma,§ Katsuhiko Nakajima,§ and Masatoshi Matsuda§

Institute for Chemical Research, Kyoto University, Uji, Kyoto 611-0011, Japan, Toyota Central R & D Labs, Inc., Nagakute, Aichi 480-1192, Japan, and Toyota Motor Corporation, Toyota, Aichi 410-1193, Japan

Received January 11, 2007; Revised Manuscript Received September 21, 2007

ABSTRACT: Effects of the crystallization temperature on the crystal structure and its melting behavior of poly (L-lactic acid) (PLLA) have been investigated by means of wide-angle (WAXS) and small-angle (SAXS) X-ray scattering, optical microscopy, and differential scanning calorimetory (DSC). PLLA was found to crystallize as the α form when the crystallization temperature T_c was higher than 120 °C, while significant change in lattice parameters was seen for T_c's below 120 °C. The ratio of the *a*- and *b*-axis lengths begins to decrease with T_c below 120 °C and is $3^{1/2}$ below 90 °C, which suggests a new crystalline form with hexagonal packing, namely, the α′ form. The possible reason for α′ formation is discussed. High-temperature WAXS and SAXS measurements showed that α′ crystal transforms into ordered *a* form during heating. The transition takes place at 150 °C without a decrease in scattering intensity and without heating rate dependence. The mechanism for the transition is discussed.

1. Introduction

Poly(L-lactic acid), PLLA, is attracting much attention, particularly from the ecological point of view due to the producibility from renewable resources. Because of its biodegradable property, PLLA is expected to be used for medical devices such as controlled drug release matrixes. It is known that the rate of hydrolytic degradation of PLLA is strongly affected by the degree of crystallinity.[1,2] Therefore, it is well expected that the solid-state structure including a crystalline lamellar organization plays an important role for controlling the degradation rate. The study on the crystallization of PLLA is, thus, of great important not only from academic interest but also from the engineering viewpoint.

Despite extensive studies of PLLA, its crystallization behavior, crystal structure, and melting behavior are still not completely understood. Three crystalline forms (α, *β*, and *γ*) have been reported for PLLA. Crystallization from the melt or from solution leads to α form crystal, which is the most common polymorph.[3−8] In the α form, two chains with 10_3 helical conformation are packed into an orthorhombic unit cell with dimensions of $a = 10.7$ Å, $b = 6.45$ Å, and c (fiber axis) $= 27.8$ Å.[6] The second phase, *β* form, is obtained under high drawing conditions and high temperatures.[5,9] According to the recent study by Puggiani et al., the *β* form is considered to have a frustrated structure, containing three chains in a trigonal unit cell with $a = b = 10.52$ Å and $c = 8.8$ Å.[10] Recently, Cartier et al. have reported that a third crystal modification of PLLA, *γ* form, was obtained via epitaxial crystallization on hexamethylbenzene substrate.[9] It has two antiparallel 3_1 helices packed in an orthorhombic unit cell with $a = 9.95$ Å, $b = 6.25$ Å, and $c = 8.8$ Å.

Crystallization kinetics from the melt of PLLA have been analyzed by a number of researchers. Vasanthakumari and Pennings first studied the effects of molecular weight and crystallization temperature on radius growth rate (G) and morphology of PLLA spherulites and carried out kinetics analysis based on the regime theory.[11] A peculiarity has been reported on the temperature dependence of the spherulite growth rate.[11−17] The maximum of the growth rate was observed at around 100 °C, while a second maximum was also observed at around 125 °C. The growth rate showed clear discontinuity at around 110−120 °C.[16] The appearance of the discontinuity is reported to be dependent on the molecular weight,[14,15] tacticity,[15] and species for copolymerization.[15] This behavior has been explained by the regime transition from II to III[14,15] since the slope ratio in the Hoffman−Lauritzen analysis was very close to 2. However, other explanations have also been reported recently from several research groups.[16−18] The origin of the peculiarity is still under open question and is required to investigate for an understanding of overall crystallization behavior of PLLA.

Most possible explanation might be the difference in the crystal modification, which was recently proposed by Zhang et al.[19] They investigated the effect of annealing temperature on the crystal modification of PLLA by means of infrared spectroscopy (IR) and wide-angle X-ray scattering (WAXS) and have concluded that PLLA crystallizes into a new crystal modification when it is crystallized below 120 °C. The new crystalline form was named the α′ form. It is reported to be a "disordered crystal" having the same 10_3 conformation as in α form but a loose packing manner compared to the α form. However, the details of the crystal structure of the α′ form, including lattice parameter, origin of the disorder, and condition for α′ formation, are not fully discussed.

In this paper, we first attempt to clarify the effects of crystallization temperature on the crystal structure of PLLA by means of X-ray scattering to discuss the peculiarity. We demonstrate that the limit disordered α′ form is obtained below 90 °C, which has hexagonal packing of the PLLA chain with 10_3 conformation. The origin of α′ formation will be discussed in this paper.

* Corresponding author. E-mail: kawai@pmsci.kuicr.kyoto-u.ac.jp. Phone: +81-774-38-3159. Fax: +81-774-38-3146.
† Institute for Chemical Research, Kyoto University.
‡ Toyota Central R&D Labs, Inc.
§ Toyota Motor Corporation.

10.1021/ma070082c CCC: $37.00
Published on Web 11/22/2007

It is well-known that the physical properties of semicrystalline polymer are strongly affected by the solid-state structure such as crystallinity, crystalline form, and morphology. The properties change upon heating according to structural changes, including lamellae thickening, crystal transformation, and melting.

For the thermal behavior of PLLA, structural changes in the PLLA crystal during heating has been briefly reported.[8,20,21] Zhang et al. also reported the crystal transformation from α′ to α, but the mechanism of the transformation is not sufficiently discussed.[19] In the present study, we report on the structural change during the heating of PLLA crystallized at various temperatures from the melt and are going to show that the transformation from α′ to α takes place possibly via a solid-phase transition.

2. Experimental Section

Poly(L-lactic acid) (PLLA) used in this study was supplied by Toyota Motor Corporation. The weight-averaged molecular weight and the molecular weight distribution were determined by GPC as 206 000 and 2.9, respectively. The optical purity was 98.4%.

PLLA was melted and pressed into sheets at 200 °C for 2 min to erase previous thermal history, followed by quenching in another oven for isothermal crystallization. After completion of the crystallization, the sample was again subjected to quenching in ice water to fix the crystal structure.

The spherulite growth in the film was observed using a Nikon polarization microscope (Optiphot2-POL) equipped with a home built temperature jump stage and a temperature controller.

Wide-angle X-ray scattering (WAXS) measurements were carried out at room temperature using a Rigaku RINT-2000 diffractometer. A monochromatized Cu Ka beam (40 kV, 30 mA) was transmitted through the sample.

High-temperature small-angle (SAXS) and wide-angle (WAXS) X-ray scattering measurements were performed using apparatuses installed at beamline BL40B2 in the SR facility, SPring-8, in Nishiharima. Wavelengths of the incident X-ray were 1.2 and 1.0 Å for SAXS and WAXS, respectively. A CCD camera (C4880: Hamamatsu Photonics K.K.) with an image intensifier was used as a detector system both for the SAXS and WAXS measurements. The q range covered in the SAXS and WAXS measurements were 0.01−0.2 and 0.2−3.0 $Å^{-1}$, respectively. The two-dimensional data were azimuthally averaged, converting the data to a one-dimensional profile. All the sample preparations and measurements above were carried out under an air atmosphere.

Thermal behavior was analyzed by a differential scanning calorimeter (DSC), Perkin-Elmer Diamond DSC, which was calibrated by the melting of indium and tin. Various heating rates (1∼20 °C/min) were applied for the samples precrystallized at 80 °C. The DSC scans were carried out in a flowing-nitrogen atmosphere.

3. Results and Discussions

3.1. Crystallization Behavior of PLLA. In Figure 1, spherulite growth rate, G, is plotted against the crystallization temperature, T_c. It is well-known that the crystal growth rate shows a bell-shaped temperature dependence according to the crystallization theory. It has been reported for many polymers including nylon-6,[22] poly(ethylene terephthalate),[23] and isotactic polystyrene[24] that the value of G increases with T_c, and after reaching the maximum it then decreases with increasing T_c. PLLA, however, shows discontinuity in the growth rate as shown in Figure 1. The spherulite growth rate curve displays a first maximum at around 130 °C and a second at around 105 °C.

The kinetic data obtained from Figure 1 have been examined in terms of secondary nucleation theory. The general expression

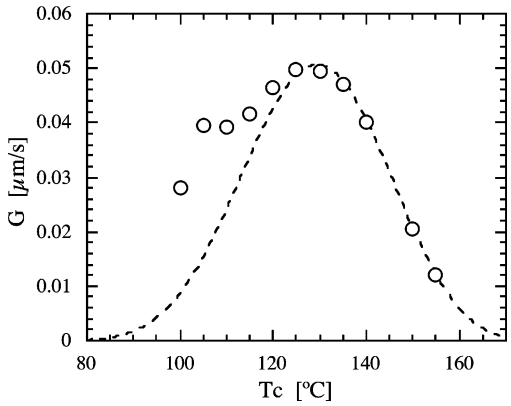

Figure 1. Radius growth rate G of the spherulite of PLLA as a function of crystallization temperature (T_c). The broken line indicates the theoretical curve fitted for the temperature above 120 °C based on the Hoffmann−Lauritzen analysis (see text).

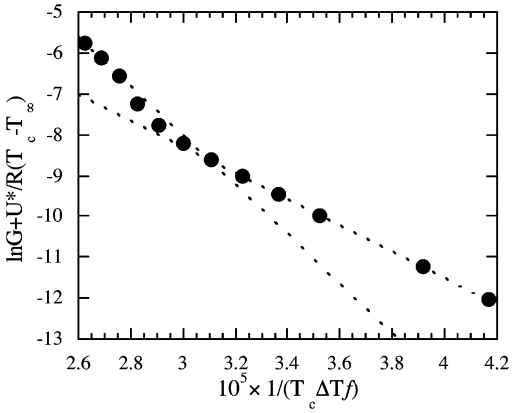

Figure 2. Hoffman−Lauritzen analysis of spherulite growth rate data of PLLA.

for the growth rate of a linear polymer crystal with a folded chain is given by

$$G = G_0 \exp\left(\frac{-U^*}{R(T_c - T_\infty)}\right) \exp\left(\frac{-K_g}{T_c \Delta T f}\right) \qquad (1)$$

where K_g is the nucleation constant, ΔT is the degree of undercooling defined by $T^\circ_m - T_c$; T°_m is the equilibrium melting point, f is a factor given as $2T_c/(T^\circ_m + T_c)$, U^* is the activation energy for segment diffusion to the site of crystallization, R is the gas constant, T_∞ is the hypothetical temperature where all motions associated with viscous flow cease ($T_g \sim -30$ K), and G_0 is the front factor. For the calculations, literature values of $T^\circ_m = 215$ °C and $T_g = 62.5$ °C were used.[14] To fit experimental data, $U^* = 1500$ cal/mol was utilized, as done in previous studies on PLLA.[25]

The results of the kinetic data treatment, using G values presented in Figure 1, are illustrated in Figure 2. The plot gives K_g as a slope and the intercept ln G_0. One can see clearly that data are composed of two lines having different slopes. The temperature of intersection was determined to be 120 °C. K_g values are estimated to be 6.02×10^5 and 3.22×10^5 K^2 for below and above 120 °C, respectively, which are close to the value previously reported.[15]

This "discontinuity" has been reported by a number of researchers. It is known that the discontinuity is dependent on the molecular weight,[14,15] incorporated comonomer unit,[15] and tacticity.[15] This phenomenon has been assumed to be of a regime transition.[14,15] Abe et al. have first analyzed the kinetic data by means of regime theory and have investigated that the regime

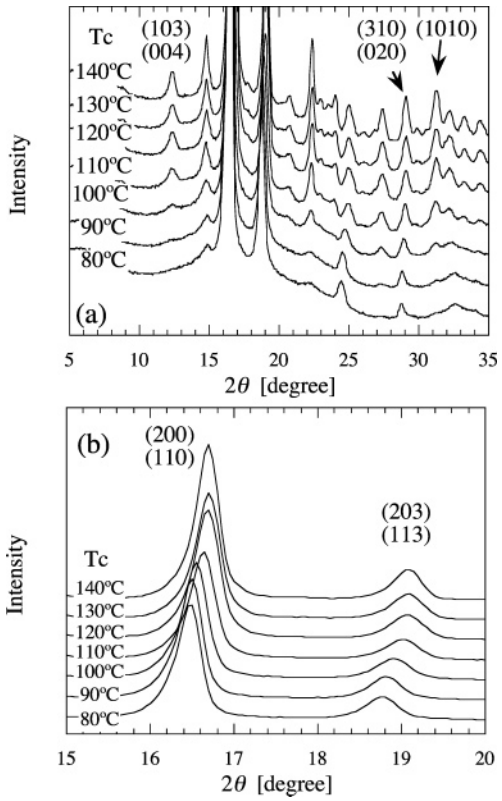

Figure 3. WAXS profiles of the sample crystallized at various T_c's from the melt.

transitions, from regime III to regime II and from regime II to regime I, occur at 120 °C and 147 °C, respectively.[15] They observed clear morphological change at 147 °C, which PLLA forms hexagonal-shaped single crystals above the temperature and three-dimensional spherulite growth below it. It is important to note that they did not observe any morphological change at 120 °C (lower transition temperature), although it is assumed to be a regime III to regime II transition.

Di Lorenzo has recently claimed on the regime transition mechanism because of (i) no morphological change at around 120 °C and (ii) two distinct straight lines below 120 °C in the Hoffmann−Lauritzen treatment.[16] According to the Raman spectroscopic study recently published by Zhang et al., the chain packing is slightly different when PLLA is crystallized at a different temperature.[19]

Detailed study about the crystallization temperature dependence on the crystal structure of PLLA is now necessary to discuss the discontinuity in crystallization kinetics. In the next section, we attempt to clarify the effect of crystallization temperature on the crystal structure of PLLA.

3.2. Crystal Structure of PLLA. Figure 3 shows the WAXS profile of the samples crystallized at various temperatures from the melt. For T_c's above 120 °C, the most intense peak is observed at a 2θ value of 16.70° that is attributed to (110) and/or (200) planes. For T_c's above 120 °C, the profiles are assigned to be the α form PLLA, which is orthorhombic with parameters $a = 10.7$ Å, $b = 6.45$ Å, and c (fiber axis) $= 27.8$ Å, where the molecules are assumed to have a left-handed 10_3 helical conformation.[6] For T_c's lower than 120 °C, however, one can find two peculiarities, which are (i) the absences of some diffractions and (ii) the 2θ shifts in every diffraction.

Despite the fact that diffraction intensity from (200)/(110) at 16.50° is not greatly different in each of the T_c's, some diffractions including (103) and (1010) are completely absent

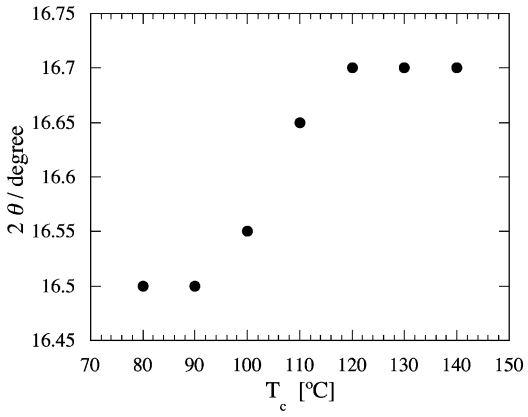

Figure 4. 2θ values from (200)/(110) diffractions of PLLA crystallized at various T_c's from the melt.

Table 1. Lattice Parameters of PLLA Crystallized at Two Different Temperatures

T_c [°C]	a [Å]	b [Å]	a/b
90	10.74	6.20	1.73
140	10.6	6.00	1.77

at lower temperatures below 90 °C. It suggests that the lack of some diffractions are not due to the decrease in crystallinity with decreasing T_c, but the crystal structure for lower T_c's is not the same as the α form at higher T_c's.

In addition to the lack of diffractions, each crystalline peak changes its position when T_c is lower than 120 °C. Figure 4 shows the plot of Bragg angles of (200)/(110) against the crystallization temperature. A Bragg angle above 120 °C stays constant at 16.70°, which agrees well with the α form crystal, while it stays constant also but with a different angle ($2\theta = 16.50°$) for lower T_c's below 90 °C. The difference is very small but promising since the other diffractions including (130)/(020) exhibit the same T_c dependences. We tried further analysis on the difference of the crystal structure.

Table 1 shows the lattice parameters derived from the WAXS profile for the samples crystallized at 80 °C (α′ form) and 140 °C (α form). Both *a*- and *b*-axis lengths of the α′-form is slightly longer (approximately 1%) than those of the α form. Surprisingly, the ratio between *a*- and *b*-axis lengths for the α′-form is 1.732, i.e., $3^{1/2}$. This means that the distances between the neighboring chain are identical, suggesting hexagonal packing of PLLA chains at lower T_c's. It seems to be secure to assume that the α′ form has a hexagonal packing since the absence of some diffractions is well explained by the extinction rule of the hexagonal lattice ($-h + k + l \neq 3n$). It is also found that the peak shift of (116)/(206) is due to the change in lattice parameters only in the *ab* plane. It means, thus, that *c*-axis length stays constant at 28.8 Å, suggesting that the chain conformation of the PLLA chain is not greatly different in each crystal except some distortions in the 10_3 helical conformation. The new crystal form is, thus, interpreted as a pseudo-hexagonal unit cell with parameter $a = b = 6.2$ Å whereas the *c*-axis coincides with that of the α form ($c = 28.8$ Å). Zhang et al. have concluded from IR measurements that the PLLA chain has the same 10_3 helical conformation for all T_c's when it is crystallized from the melt.[19,26] They precluded the possibility of β phase formation at low T_c's, which have been proposed by Kawaguchi et al.,[18] since the chains in the β phase have 3_1 helical conformations. Our WAXS results are consistent with their IR results, indicating new crystal modification.

What could be the reason for the pseudo-hexagonal phase formation at low temperature? We assume that a certain

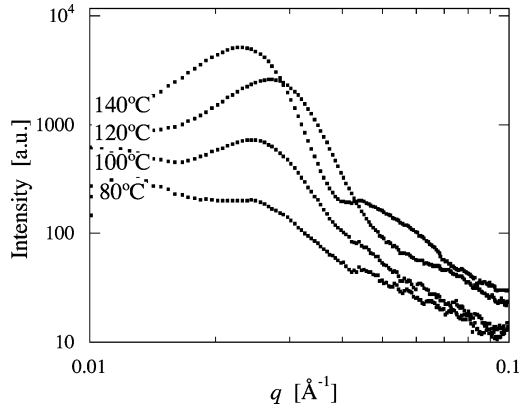

Figure 5. SAXS profiles of PLLA crystallized at various T_c's from the melt.

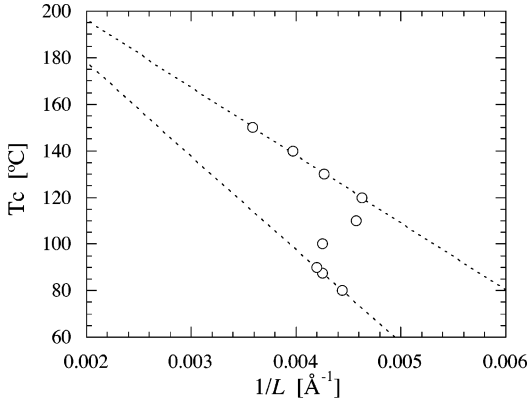

Figure 6. Relation between the inverse long period, $1/L$, and the crystallization temperature, T_c.

disorder plays an important role to form the pseudo-hexagonal crystal.

It has been reported that some kind of disorder gives rise to the formation of the pseudo-hexagonal crystal or "solid mesophase".[27] Random copolymer of ethylene with propylene (EP), with propylene content around 25%, is known to crystallize into a pseudo-hexagonal lattice by melt-crystallization[28,29] and/or mechanical stretching.[30,31] It is considered that the propylene units are included in the crystalline lattice of the orthorhombic form of polyethylene (PE, $a = 7.42$, $b = 4.95$, $c = 2.54$ Å),[32] leading to pseudo-hexagonal packing due to the large amount of disorder within the orthorhombic lattice. One should be reminded that the a/b ratio of the α form crystal of PLLA is close to $3^{1/2}$, indicating very weak anisotropy in its packing manner in the *ab* plane. Although PLLA has no noncrystallizable unit in its chain, chain distortion could play an important role for the formation of hexagonal packing. Sasaki et al. have reported that the 10_3 helical conformation of the PLLA chain is periodically distorted when it is crystallized at 90 °C.[7] This helical distortion may relieve the anisotropy in the chain packing in the *ab* plane, inducing a pseudo-hexagonal crystal without change in the *c*-axis length.

The rotational disordering could be one of the possibilities to make the hexagonal phase happen. It is well-known that polyethylene crystallizes into the pseudo-hexagonal form at high pressure and temperature.[33−36] The hexagonal structure containing a high amount of structural disorder has been proposed for this intermediate form of PE. This kind of disordering may cause the formation of the hexagonal phase of PLLA.

Another possibility is based on the statistical disorder of the up and down chains in the crystalline lattice. The structure of the α-form isotactic polypropylene (iPP) may be described with reference to a limit ordered model.[27] iPP has two variants in the α form, which are perfectly ordered crystalline phase (α_2 form) with the order of an up/down 3_1 helix and less ordered α_1 form with statistical disorder in the chain direction.[37,38] In the α form of PLLA as a perfect ordered model, up and down 10_3 helixes are considered to be packed alternatively. It is possible to assume, like in iPP, that the statistical disorder in an up/down helix may introduce a limit-disordered crystal with a pseudo-hexagonal lattice.

The evidence of the formation of a new crystal modification at low T_c's is also obtained from SAXS measurements. Figure 5 shows SAXS profiles of the sample crystallized at various T_c's from the melt. The profiles are taken at the crystallization temperatures since the scattering intensity is too weak at room temperature to detect, possibly due to the difference in the temperature dependence of the density between the crystalline phase and the amorphous phase. The intensity maximum at q_{max}, which relates to the long spacing ($L = 2\pi/q_{max}$), can be seen at each T_c, while a peculiarity is observed regarding the T_c dependence of long spacing. In Figure 6 relations between T_c and the inverse long spacing, $1/L$, are shown as a Gibbs−Thomson type plot. One can see clearly that there are two T_c dependences in inverse long spacing. All the points above 120 °C are well on the line, suggesting single-crystal modification in this temperature range. It agrees well with the WAXS result, which only the α form crystal was observed. When it is crystallized below 90 °C, on the other hand, all points show monotonous T_c dependence but are on another line. It indicates clearly that formation of the lamellae structure is governed by a different mechanism according to the temperature range. As we described before, PLLA chains crystallize into a hexagonal crystal (α′ form) when T_c is below 90 °C. The line in this temperature range, thus, indicates the T_c dependence of the α′ form crystal. Zhang et al. have revealed that the α′ form is obtained below 120 °C,[19] while our detailed analysis based on both WAXS and SAXS made it possible to understand that the "pure" α′ form, which might be a limit disordered crystal with hexagonal packing of the 10_3 helix of the PLLA chain, is obtained only when T_c is below 90 °C.

When the crystallization takes place at the temperatures ranging from 90 to 120 °C, inverse long spacing shows peculiar T_c dependence. It shows the long spacing decreases with increasing crystallization temperature. It seems that the inverse long spacing changes from the α form line to that of the α′ form with decreasing crystallization temperature. This unique behavior may be interpreted as following two different models: (i) mixture model of two variant crystals (α form and α′ form), where the α form and the α′ form crystal coexist with a certain volume fraction depending on its crystallization temperature or (ii) the statically disordered model, where the degree of disorder in the crystal changes with temperature. This problem is still an open question, and further study is required.

3.3. Melting Behavior of PLLA. Parts a and b of Figure 7 show the changes in the WAXS profile upon heating at 10 °C/min for the sample crystallized at 140 °C and 80 °C, respectively. In Figure 7a ($T_c = 140$ °C), one can find both the (103)/(004) diffraction peak at 0.8 $Å^{-1}$ and the (1010) one at 2.4 $Å^{-1}$, which are the characteristics of the α form crystal. A slight peak shift of each diffraction has been seen upon heating due to the thermal expansion, followed by the melting at 182 °C.

Clear evidence of crystal transformation is observed upon heating when PLLA is crystallized into the α′ form ($T_c =$ 80 °C). The (103) nor the (1010) diffraction could not be seen at low temperatures below 150 °C in Figure 7b. Surprisingly, a

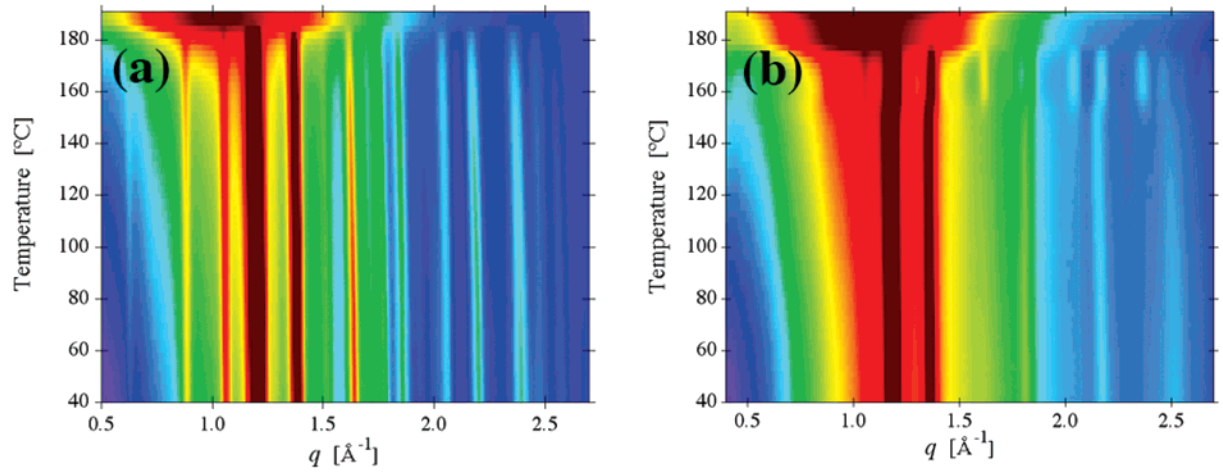

Figure 7. Changes in WAXS profiles upon heating the samples precrystallized at (a) 140 °C (α form) and (b) 80 °C (α′ form) from the melt. Heating rate is 10 °C/min.

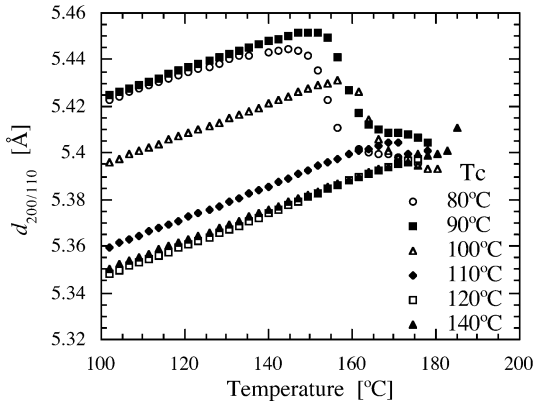

Figure 8. Change in (110)/(200) lattice spacing upon heating the sample crystallized at various temperatures.

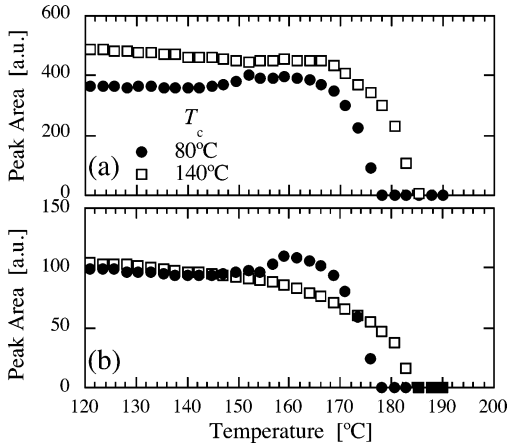

Figure 9. Change in peak area of (a) (110)/(200) and (b) (020)/(130) upon heating.

sudden peak shift is observed at 150 °C. Additional diffractions such as (103) and (1010) appear above the temperature. It indicates the change in the space group of the PLLA crystal, in other words, the change in crystalline form. The profiles above 150 °C are identical for both T_c's, suggesting that the α′ form crystal suffers from transformation into the α form. This transformation is needed to investigate in detail.

Figure 8 indicates the change in the (110)/(020) lattice spacing upon heating. The lattice spacing increases linearly with temperature in the whole range (100−180 °C) when T_c is above 120 °C. It is important to note that the lattice spacing shows drastic change when T_c is below 120 °C. The samples crystallized below 120 °C have different lattice parameters at room temperature, depending on its crystallization temperature as already indicated in Figure 4. It is seen that the slope of the linear increase in $d_{110/020}$ for the T_c lower than 120 °C is almost parallel to that of the α form PLLA. It means that the thermal expansions for both the α and α′ crystals are nearly equal, suggesting the chain packing manners are very close. For further heating, $d_{110/020}$ decreases with temperatures above 150 °C toward that of the α form. This strongly suggests that the transition from the α′ to the α form takes place at this temperature.

Figure 9 shows the change in the peak area of diffractions from (a) (110)/(200) and (b) (130)/(020) during the heating. The area of the α form crystal (T_c = 140 °C) stays almost constant until it starts to melt at 170 °C, suggesting constant crystallinity upon heating. On the other hand, the α′ form (T_c = 80 °C) shows increase above 150 °C, followed by the melting. This behavior is observed in each diffraction. Considering that the lattice spacing shows drastic change at the same temperature, the increase in the diffraction intensity indicates the crystal transformation from the α′ to the α form.

Parts a and b of Figure 10 show the change in the SAXS profile upon heating for the samples crystallized at 80 °C (α′ form) and 140 °C (α form), respectively. The SAXS intensity increases with temperature for both samples. Since WAXS results showed that crystallinity stays constant during the heating of the α form below the onset temperature of melting at 170 °C, we consider that the increase in the SAXS intensity is originated in the increasing density difference between the crystalline phase and the amorphous phase with increasing temperature.

SAXS invariant, Q, can be calculated from the following equation,

$$Q = \int 4\pi q^2 I(q)\, dq \qquad (2)$$

Figure 11 shows the change in Q of the samples crystallized at various temperatures from the melt during heating. For T_c's above 120 °C, Q shows monotonous increases upon heating until the steep decrease due to the melting. For T_c's below 120 °C, on the other hand, sharp increases in Q can be seen at 150 °C after a monotonous increase, which indicates the α′−α transformation.

What could be the mechanism for this transformation? From both WAXS and SAXS measurements, it is found that phase

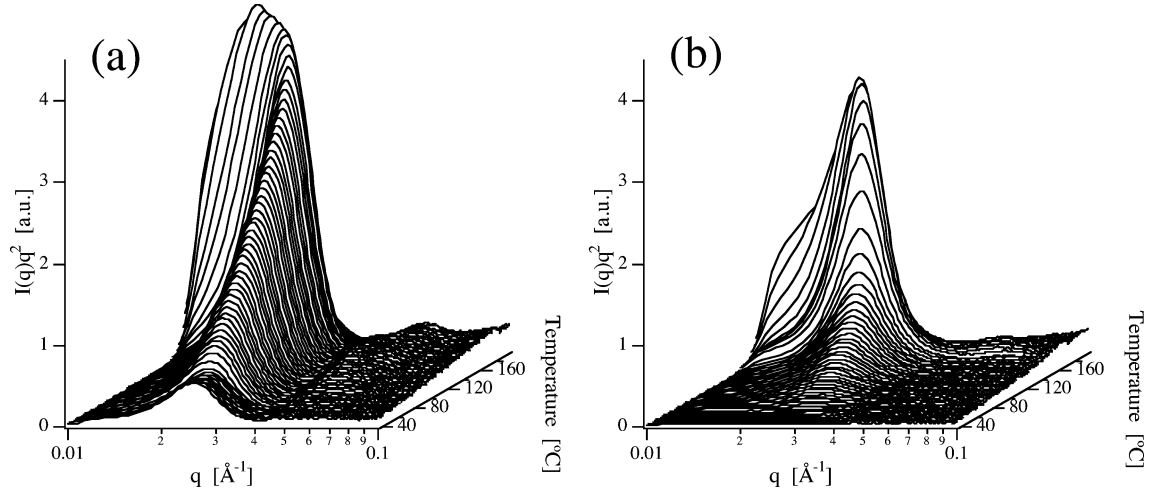

Figure 10. Change in SAXS profiles during heating the sample crystallized at (a) 140 °C and (b) 80 °C.

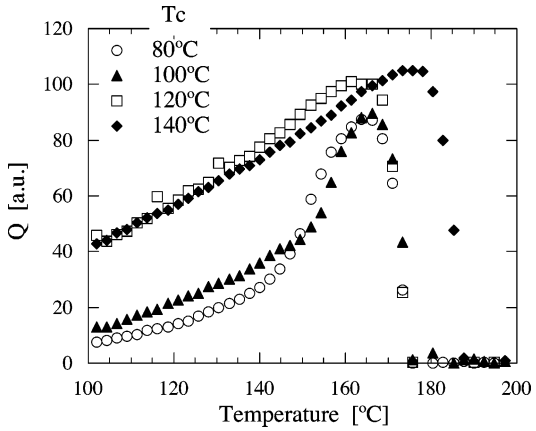

Figure 11. Change in invariant, *Q*, upon heating the sample crystallized at various temperatures.

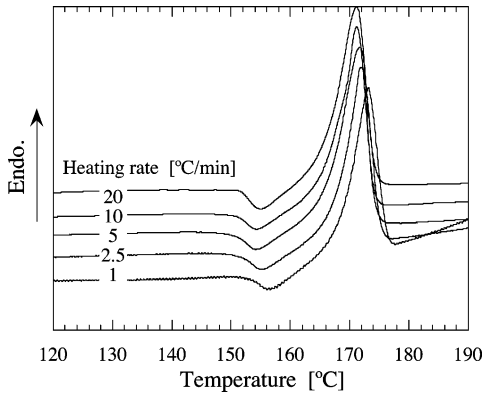

Figure 12. DSC heating thermographs of the sample crystallized at 80 °C scanned at various heating rates.

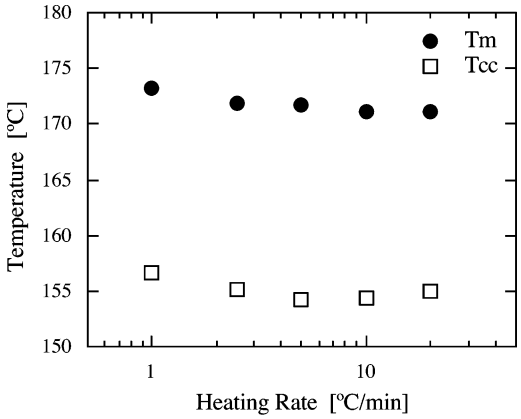

Figure 13. Effect of the heating rate on the crystallization temperature (T_{cc}) and the melting temperature (T_m) of the sample crystallized at 80 °C (α′ form).

transformation from α′ to α takes place at 150 °C prior to the melting. It must be noticed that this transformation is completed within 1.5 min (15 °C) during heating. In the case when PLLA is crystallized at 155 °C, for instance, the crystallization takes more than a day to be completed, which is very much slower than the transformation during heating. This suggests that the transformation from α′ to α is not via a simple melt−recrystallization process. In Figures 9 and 11, WAXS and SAXS measurements show no decrease in the intensities on the occasion of the phase transition at 150 °C. If the α′−α transformation proceeds via the melt−recrystallization mechanism, intensities should decrease according to the melting of the pre-existing α′ form crystal, followed by an increase due to the recrystallization process into the ordered α crystal. This behavior suggests the transformation without the melting process, i.e., the solid−solid-phase transition.

Figure 12 shows DSC thermographs of PLLA crystallized at 80 °C from the melt. The heating rates are ranging from 1 to 20 °C/min, and the measurement was carried out immediately after the completion of the crystallization. It is important to note that the exothermic peak appears prior to the melting peak for all heating rates. It indicates that the crystallization occurs before the melting process. For the heating rate of 10 °C/min, the crystallization starts at 150 °C, which shows very good agreement with WAXS and SAXS measurements. This crystallization peak indicates, thus, the crystal transformation from the α′ form to the α form, again confirming the solid−solid-phase transition.

In Figure 13, the melting peak temperatures (T_m) and the crystallization peak temperatures (T_{cc}) are plotted against the heating rate. It is well-known that the DSC thermograph changes its shape with the heating rate if the crystal transformation is governed by the melt−recrystallization mechanism, since the recrystallization process requires suitable time for crystallization into another crystalline form. The α′ form of PLLA, however, shows almost no heating rate dependence. Within the limited experimental heating rate, both the crystallization peak temperatures and the melting peak temperatures stay constant. The above finding leads us to propose that the transition is without melting, i.e., solid−solid phase transition.

4. Conclusion

We report on the effect of crystallization temperature on the crystal structure and melting behavior of PLLA, studied with temperature-resolved synchrotron WAXS and SAXS as well as DSC. We have shown three new findings in the crystallization and melting behavior of PLLA, which are (i) α′ crystal formation below $T_c = 90$ °C that is a limit disordered crystal, (ii) the α′ form as a hexagonal phase, and (iii) the α′−α transition without the melting−recrystallization process (solid-phase transition).

PLLA was found to crystallize as the α form when the crystallization temperature was higher than 120 °C, while a significant change in the lattice parameters was seen for lower T_c's below 120 °C. The ratio of the *a*- and *b*-axis length begins to decrease above 120 °C and is $3^{1/2}$ below 90 °C, which suggests a new crystalline form with hexagonal packing, namely, the α′ form. Analyzing the WAXS and SAXS data, we demonstrated that the "pure" α′ form was obtained when the crystallization temperature is below 90 °C. The α′ form is proposed to be a limit disordered crystal with hexagonal packing.

We also studied the melting behavior of the α and α′ forms of PLLA using WAXS, SAXS, and DSC and found that the disordered-type α′ form transformed into the ordered-type α form crystal during heating. The transition occurs at 150 °C, which agrees well with the onset temperature of the exothermic peak in the DSC measurement. We found that the transition proceeds without the melting process in a very short time. The above finding strongly suggests the α′−α transition is a solid−solid-phase transition.

References and Notes

(1) Cam, D.; Hyon, S. H.; Ikada, Y. *Biomaterials* **1995**, *16*, 833.
(2) Tsuji, T.; Nakahara, K.; Ikarashi, K. *Macromol. Mater. Eng.* **2001**, *286*, 398.
(3) Miyata, T.; Masuko, T. *Polymer* **1997**, *38*, 4003.
(4) De Santis, P.; Kovacs, A. J. *Biopolymer* **1968**, *6*, 299.
(5) Hoogsteen, W.; Postema, A. R.; Pennings, A. J.; ten Brinke, G.; Zugenmaier, P. *Macromolecules* **1990**, *23*, 634.
(6) Kobayashi, J.; Asahi, T.; Ichiki, M.; Okikawa, A.; Suzuki, H.; Watanabe, T.; Fukuda, E.; Shikinami, Y. *J. Appl. Phys.* **1995**, *77*, 2957.
(7) Sasaki, S.; Asakura, T. *Macromolecules* **2003**, *36*, 8385.
(8) Brizzolara, D.; Cantow, H. J.; Diederichs, K.; Keller, E.; Domb, A. J. *Macromolecules* **1996**, *29*, 191.
(9) Cartier, L.; Okihara, T.; Ikada, Y.; Tsuji, H.; Puiggali, J.; Lotz, B. *Polymer* **2000**, *41*, 8909.
(10) Puiggali, J.; Ikada, Y.; Tsuji, H.; Cartier, L.; Okihara, T.; Lotz, B *Polymer* **2000**, *41*, 8921.
(11) Vasanthakumari, R.; Pennings, A. J. *Polymer* **1983**, *24*, 175.
(12) Tsuji, H.; Takai, H.; Saha, S. K. *Polymer* **2006**, *47*, 3826.
(13) Tsuji, H.; Miyase, T.; Tezuka, Y.; Saha, S. K. *Biomacromolecules* **2005**, *6*, 244.
(14) Abe, H.; Kikkawa, Y.; Inoue, Y.; Doi, Y. *Biomacromolecules* **2001**, *2*, 1007.
(15) Tsuji, H.; Tezuka, Y.; Saha, S. K.; Suzuki, M.; Itsuno, S. *Polymer* **2005**, *46*, 4917.
(16) Di Lorenzo, M. L. *Eur. Polym. J.* **2005**, *41*, 569.
(17) Yasuniwa, M.; Tsubakihara, S.; Iura, K.; Ono, Y.; Dan, Y.; Takahashi, K. *Polymer* **2006**, *47*, 7554.
(18) Ohtani, Y.; Okumura, K.; Kawaguchi, K. *J. Macromol. Sci. Phys.* **2003**, *3−4*, 875.
(19) Zhang, J.; Tashiro, K.; Domb, A. J.; Tsuji, H. *Macromol. Symp.* **2006**, *242*, 274.
(20) Cho, T. Y.; Strobl, G. *Polymer* **2006**, *47*, 1036.
(21) Mano, J. F.; Wang, Y.; Viana, J. C.; Denchev, Z.; Oliveira, M. J. *Macromol. Mater. Eng.* **2004**, *289*, 910.
(22) Burnett, B. B.; McDevit, W. F. *J. Appl. Phys.* **1957**, *28*, 1101.
(23) van Antwerpen, F.; van Krevelen, D. W. *J. Polym. Sci., Part B* **1972**, *10*, 2423.
(24) Suzuki, T.; Kavacs, A. J. *Polym. J.* **1970**, *1*, 82.
(25) Iannace, S.; Nicolais, L. *J. Appl. Polym. Sci.* **1997**, *64*, 911.
(26) Zhang, J.; Duan, Y.; Sato, H.; Tsuji, H.; Noda, I.; Yan, S.; Ozaki, Y. *Macromolecules* **2005**, *38*, 8012.
(27) Auriemma, F.; De Rosa, C.; Corradini, P. *Adv. Polym. Sci.* **2005**, *181*, 1.
(28) Wunderlich, B.; Poland, D. *J. Polym. Sci., Part A* **1963**, *1*, 357.
(29) Eichhorn, R. M. *J. Polym. Sci.* **1958**, *31*, 197.
(30) Bassi, I. W.; Corradini, P.; Fagherazzi, G.; Valvassori, A. *Eur. Polym. Sci.* **1970**, *6*, 709.
(31) Scholtens, B. J. R.; Riande, E.; Mark, J. E. *J. Polym. Sci., Polym. Phys. Ed.* **1984**, *22*, 1223.
(32) Bunn, C. W. *Trans. Faraday Soc.* **1939**, *35*, 482.
(33) Bassett, D. C.; Block, S.; Piermarini, G. J. *J. Appl. Phys.* **1974**, *45*, 4146.
(34) Yasuniwa, M.; Enoshita, R.; Takemura, T. *Jpn. J. Appl. Phys.* **1976**, *15*, 1421.
(35) Yamamoto, T.; Miyaji, H.; Asai, K. *Jpn. J. Appl. Phys.* **1977**, *16*, 1891.
(36) Tanaka, H.; Takemura, T. *Polym. J.* **1980**, *12*, 355.
(37) Naiki, M.; Kikkawa, T.; Endo, Y.; Nozaki, K.; Yamamoto, T.; Hara, T. *Polymer* **2000**, *42*, 5471.
(38) Mencik, Z. *J. Macromol. Sci. Phys.* **1972**, *B6*, 101.

MA070082C